Electrospun Polyacrylonitrile Nanofibers Containing a High Concentration of Well-Aligned Multiwall Carbon Nanotubes

Haoqing Hou,*,†,‡ Jason J. Ge,‡ Jun Zeng,§ Qing Li,‡ Darrell H. Reneker,*,‡ Andreas Greiner,§ and Stephen Z. D. Cheng‡

Chemistry College of Jiangxi Normal University, Nanchang, 330027, China, Department of Polymer Science, University of Akron, Akron, Ohio 44325, and Department of Chemistry, Philipps-University Marburg, Hans-Meerwein-Str., Marburg 35032, Germany

Received September 5, 2004. Revised Manuscript Received December 10, 2004

Composite nanofiber sheets of well-aligned polyacrylonitrile nanofibers (PAN) containing multiwall carbon nanotubes (MWCNTs) were prepared by electrospinning a MWCNT-suspended solution of PAN in dimethyl formamide using a moving collector. Scanning electron microscopy, atomic force microscopy, transmission electron microscopy (TEM), IR spectroscopy, Raman spectroscopy, X-ray scattering, and the Instron test were used to characterize the nanofiber sheets. TEM observation showed the MWCNTs were parallel and oriented along the axes of the nanofibers. The mechanical properties of the composite nanofibers were reinforced by MWCNT fillers. Carbonization processes showed that a higher concentration of MWCNTs effectively resisted heat shrinkage of the composite nanofiber sheet.

1. Introduction

Electrospinning is one of the effective methods to produce polymer nanofibers,[1−4] which have been successfully used as filters for air filtration,[5] as templates for making tubular nanostructures such as metal nanotubes,[6] metal oxide nanotubes[7,8] or polymer nanotubes,[6,9] and as substrates for forming hierarchical carbon nanostructures.[10] Electrospun nanofibers are also finding uses in protective clothing,[11] nanocomposites,[12] optical sensors,[13] biomedical applications including biomedicine,[14−16] scaffolding for tissue growth,[17,18] drug delivery systems,[19] and for solar sails in space.[20] For macroscopic applications such as clothing, solar sails in space, or media for filtration, stronger polymer nanofibers are desired. However, the polymer nanofibers produced by electrospinning processes are not as strong as desired due to their very small diameters and the unoptimized molecular orientation in the fibers. Stretching and making composites can improve the mechanical properties of polymer fibers, but making nanocomposites is a more promising way to reinforce the nanofibers. Methods to stretch nanofibers are not available.

Carbon nanotubes (CNT), first reported by Iijima in 1990,[21] possess excellent mechanical properties and good electrical and thermal conductivity, making CNTs an ideal material for reinforcing polymer materials. Several reports were published on polymer materials reinforced by using CNTs.[22−26] The modulus and tensile strength were improved from several percent up to more than 100 percent, depending

* Corresponding authors: haoqing@jxnu.edu.cn (H.H.); dhr@polymer.uakron.edu (D.H.R.).
† Jiangxi Normal University.
‡ University of Akron.
§ Phillips-University Marburg.

(1) Baumgarten, P. K. *J. Colloid Interface Sci.* **1971**, *36*, 71.
(2) Jaeger, R.; Schoenherr, H.; Vansco, G. J. *Macromolecules* **1996**, *29*, 7634.
(3) Reneker, D. H.; Chun, I. *Nanotechnology* **1996**, *7*, 216.
(4) Reneker, D. H.; Yarin, A. L.; Fong, H.; Koombhongse, S. J. *J. Appl. Phys.* **2000**, *87*, 4531.
(5) Graham, K.; Ouyang, M.; Raether, T.; Grafe, T.; McDonald, B.; Knauf, P. *The Fifteenth Annual Technical Conference & Expo of the American Filtration & Separations Society*; Galveston: Texas, 2002; April 9−12.
(6) Bognitzki, M.; Hou, H.; Ishaque, M.; Frese, T.; Hellwig, M.; Schwarte, C.; Schaper, A.; Wendorff, J. H.; Greiner, A. *Adv. Mater.* **2000**, *12*, 637.
(7) Liu, W.; Graham, M.; Evans, E. A.; Reneker, D. H. *J. Mater. Res.* **2002**, *17* (12), 3206.
(8) Caruso, R. A.; Schattka, J. H.; Greiner, A. *Adv. Mater.* **2001**, *13*, 1577.
(9) Hou, H.; Zeng, J.; Reuning, A.; Schaper, A.; Wendorff, J. H.; Greiner, A. *Macromolecules* **2002**, *35*, 2429.
(10) Hou, H.; Reneker, D. H. *Adv. Mater.* **2004**, *16*, 69.
(11) Gibson, P.; Schreuder-Gibson H.; Rivin, D. *Colloids Surf. A* **2001**, *187−188*, 469.
(12) Bergshoef, M. M.; Vancso, G. J. *Adv. Mater.* **1999**, *11*, 1362.
(13) Wang, X.; Drew, C.; Lee, S.-H.; Senecal, K. J.; Kumar, J.; Samuelson, L. A. *Nano Lett.* **2002**, *2* (11), 1273.
(14) Stizel, J. D.; Bowlin, G. L.; Mansfield, K.; Wnek, G. E.; Simposon, G. Electrospraying and Electrospinning of Polymer for Biomedical Applications. Poly(lactic-co-glycolic acid) and Poly(ethylene-co-vinylacetate). Presented at *32nd International SAMPE Technology Conference*; Boston, MA, November 5−9, 2000.
(15) Smith, D.; Reneker, D. H.; Kataphinan, W.; Dabney, S. *PCT Int. Appl. WO 2000-US27775*; 2001.
(16) Smith, D.; Reneker, D. H. *PCT Int. Appl. WO 2000-US27776*; 2001.
(17) Li, W. J.; Laurencin, C. T.; Caterson, E. J.; Tuan, R. S.; Ko, F. K. *J. Biomed. Mater. Res.* **2002**, *60* (4), 613.
(18) Matthews, J. A.; Wnek, G. E.; Simpson, D. G.; Bowlin, G. L. *Biomacromolecules* **2002**, *3*, 232−238.
(19) Kenawy, E. R.; Bowlin, G. L.; Mansfield, K.; Layman, J.; Simpson, D. G.; Sanders, E. H.; Wnek, G. E. *J. Controlled Release* **2002**, *81*, 57.
(20) White, K.; Lennhoff, J.; Sally, E.; Jayne, K. *Proceedings of The Fiber Society Annual Fall Technical Meeting*; Natick, MA, October, 2002.
(21) Iijma, S. *Nature* **1991**, *354*, 56.
(22) Gong, X.; Liu, J.; Baskaran, S.; Voise, R. D.; Young, J. S. *Chem. Mater.* **2000**, *12*, 1049.
(23) Zhang, X.; Liu, T.; Sreekumar, T. V.; Kumar, S.; Moore, V. C.; Hauge, R. H.; Smalley, R. E. *Nano Lett.* **2003**, *3* (9), 1285.
(24) Vigolo, B.; Poulin, P.; Lucas, M.; Launois, P.; Bernier, P. *Appl. Phys. Lett.* **2002**, *81* (7), 1210.
(25) Kumar, S.; Dang, T. D.; Arnold, F. E.; Bhattacharyya, A. R.; Min, B. G.; Zhang, X.; Vaia, R. A.; Park, C.; Adams, W. W.; Hauge R. H.; Smalley, R. E.; Ramesh, S.; Willis, P. A. *Macromolecules* **2002**, *35*, 9039.

10.1021/cm0484955 CCC: $30.25
Published on Web 02/02/2005

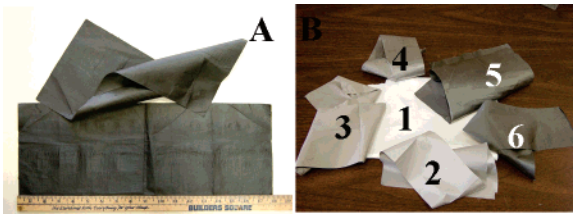

Figure 1. Optical images of electrospun composite nanofiber sheets. (A) Large sheets of 8 × 18 in.^{2} of PAN nanofibers containing MWCNTs of 10 wt %; (B) sheets of the composite nanofibers, which contain the following weight percentages: 1, 0%; 2, 2%; 3, 3%; 4, 5%; 5, 10%; 6, 20%.

on the polymer matrix, types and synthesis methods of CNT, and concentration of the CNT in the matrix. Recently, Dror et al.[27] reported electrospun polyethylene oxide nanofibers containing low concentrations of multiwall CNTs (MWCNT), which were observed using transmission electron microscopy (TEM). More recently, Ko et al.[28] reported continuous CNT-filled nanofiber yarns made by electrospinning. They found the modulus was improved 120% in nanofibers containing 4% weight concentration of single-wall CNTs (SWCNT) in the nanofibers. The tensile strength, elongation at break, and other mechanical properties were not reported.

In the work reported here, polyacrylonitrile (PAN) nanofibers containing well-aligned MWCNT with concentrations from 0 to 35 wt % were produced. Thick sheets of well-aligned nanofibers were made. This work demonstrated that, at a higher concentration, MWCNTs were nearly parallel, along the nanofiber axis, embedded within the nanofiber. The resistance of the nanofiber sheet to heat shrinkage was improved. Mechanical properties tests showed that tensile strength and modulus of the nanofiber sheet was well improved. Several sheets of PAN−MWCNT composite nanofibers are shown in Figure 1.

2. Experimental Section

Materials. PAN used in this study possessed a molecular weight of 22 600 g/mol (M_n) and 86 000 g/mol (M_w). The polymer was purchased from Aldrich. The MWCNTs were prepared on silicone substrates by vapor mixture pyrolysis of anthracene and ferrocene in an atmosphere of H_2 and Ar mixture at 700−750 °C.[29]

To uniformly disperse the MWNTs in the organic polymer matrix, the MWNTs were oxidized in a 6 M HNO_3 solution using reflux for 12 h. Carboxylic acid (−COOH) functional groups were identified on the surface of the oxidized MWNTs by fast Fourier-transform infrared (FT-IR) spectroscopy, similar to the others reported before.[30−32] Vibrational modes observed, at 3400, 1714, 957, and 920 cm^{-1}, were attributed to O−H stretching, carbonyl stretching, and out-of-plane O−H bending, respectively, which did not exist in original or purified nanotubes.[32] After chemical etching, the surface-oxidized MWNTs were well-dispersed in *N*,*N*′-dimethylformamide (DMF).

Formation of Electrospun Composite Nanofibers of PAN and MWCNT. PAN was dissolved in the stable suspension of MWCNTs in DMF at 100 °C. PAN concentration was always 7 wt % in DMF. MWCNT concentration was varied. Suspensions were prepared with MWCNT concentrations of 2, 3, 5, 10, 20, and 35% of the mass of the dissolved PAN. The electrospinning process was performed using electric fields on the order of 100 kV/m, from a 30-kV electrical potential applied to a 30-cm gap between the spinneret and a collector. The 0.16-m diameter collector rotated at a surface speed of about 10 m/s. The moving collector aligned nanofibers in the nanofiber sheet.

Characterization of Mechanical Properties of the Composite Nanofibers. Mechanical property testing was performed using a CMT-8500 Electromechanical Universal Testing Machine (SAMS company). The samples were prepared in 2 mm width and 60 mm length. The cross section of the sample was calculated via the weight of the sample and the densities of PAN and MWCNT. The density of PAN is 1.2 g/cm^3, and that of MWCNT is 1.8 g/cm^3.

Carbonization of PAN−MWCNT Composite Nanofibers. The carbonization of the PAN−MWCNT composite nanofiber sheet was performed in a tubular quartz reactor (inner diameter 60 mm, effective heating length 650 mm). First, oxidative stabilization of the nanofiber sheet was completed at 220 °C in air for 2 h. In this treatment, thermoplastic PAN was converted to a nonplastic cyclic or ladder compound.[33] Then the samples was heated from 220 to 850 °C at a heating rate of 2 °C/min in an atmosphere of Ar and stayed at the last temperature for a half hour.

Electron Microscopy. The morphology and diameter of Pt sputter-coated neat or composite nanofibers was evaluated using JEOL JSM-5310 scanning electron microscopy (SEM) at 25 kV. A Philips TECNAI transmission electron microscope was utilized to study the size, distribution, and structure of carbon nanotubes in the composite nanofibers on 200-mesh Cu grids with an accelerating voltage of 120 kV. Both the bright-field images and the selected-area electron diffraction patterns of the nanofibers were obtained. Calibration of the diffraction pattern was done using TiCl *d* spacings and their higher order diffractions.

Atomic Force Microscopy (AFM). An atomic force microscope (Veeco Digital Instrument Nanoscope IIIA) was utilized to map the surface topology of nanofibers. Tapping mode was used for the nanofibers on fresh cleaved mica substrates at ambient temperature to obtain both phase and height images. The scanner was calibrated in both lateral and vertical directions using the standard grid. A typical measurement condition was as follows: scan size of ~2 μm, scan rate of ~0.7 Hz, operation and resonance frequency of ~300 kHz, and resolution of ~512 × 512 lines.

Raman Spectroscopy and X-ray Diffraction. Raman spectroscopy was performed using a Jobin-Yvon LABRAM HR800 with 514.5-nm Ar laser excitation. Wide-angle X-ray diffraction (WAXD) was performed with a Siemens D5000 using Cu Kα radiation.

IR Spectroscopy. Fast Fourier transfer infrared (FT-IR) spectra of carbon nanotube samples were measured with a Digilab Win-IR Pro Instrument in a transmission mode at room temperature. The carbon nanotubes were dispersed into tetrahydrofuran (THF) by sonication for 30 min. Then the carbon nanotube solution was cast on transparent NaCl crystal plates. The resolution for FT-IR was at 4.0 cm^{-1}. Nicolet Nexus 870 attenuated total reflection (ATR) FT-IR was also used to directly analyze the surfaces of

(26) Thostenson, E. T.; Chou, T.-W. *J. Phys. D: Appl. Phys*. **2002**, *35*, L77.
(27) Dror, Y.; Salalha, W.; Khalfin, R. L.; Cohen, Y.; Yarin, A. L.; Zussman, E. *Langmuir* **2003**, *9*, 7012.
(28) Ko, F.; Gogotsi, Y.; Ali, A.; Naguib, N.; Ye, H.; Yang, G.; Li, C.; Willis, P. *Adv. Mater.* **2003**, *15* (14), 1161.
(29) Hou, H.; Schaper, A.; Weller, F.; Greiner, A. *Chem. Mater*. **2002**, *14*, 3990.
(30) Chen, J.; Hamon, M. A.; Hu, H.; Chen, Y.; Rao, A. M.; Eklund, P. C.; Haddon, R. C. *Science* **1998**, *282*, 95.
(31) Kovtyukhova. N. I.; Mallouk, T. E.; Pan, L.; Dickey, E. C. *J. Am. Chem. Soc*. **2003**, *125*, 9761.
(32) Chen, R. J.; Zhang, Y.; Wang, D.; Dai, H. *J. Am. Chem. Soc*. **2001**, *123*, 3838.
(33) Inagaki, M. *New Carbons: Control of Structure and functions*; Elsevier: Oxford, UK, 2000; p 85.

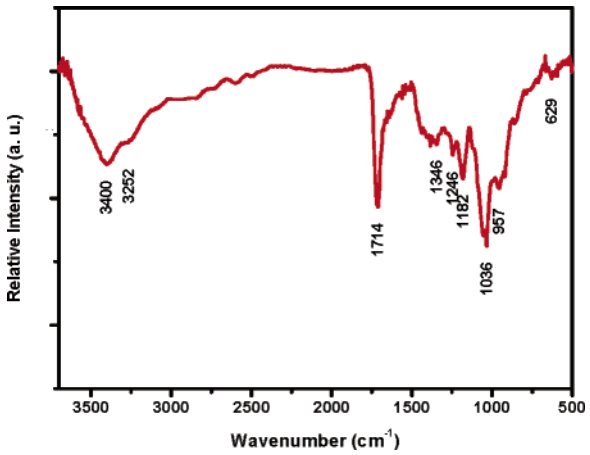

Figure 2. IR spectra of the MWCNT modified with carboxyl groups.

carbon nanotubes with a high-resolution Ge single-crystal detector (up to 1.0 cm^{-1}).

3. Results and Discussion

3.1. Formation of PAN−MWCNT Composite Nanofibers. PAN was selected as a suitable matrix of MWCNT for making composite nanofibers since: (1) it is soluble in solvent DMF, which is also a good solvent for suspending MWCNTs that were surface-modified with carboxylic groups; (2) it is a well-known precursor for making carbon fibers. For purification, the as-synthesized MWCNTs[29] were treated by reflux in 6 M HNO_3 for 12 h followed by filtration and a wash with deionized water. IR spectroscopy (Figure 2) showed that the surface of MWCNT was modified with carboxylic groups during the course of refluxing in 6 M HNO_3 solution. The result agreed with the work reported previously.[30] The cleaned, dried modified MWCNTs were observed using TEM as shown in Figure 3A. The HRTEM images (parts B and C of Figure 3) showed that the surface of the modified MWCNT was similar to that of nonmodified MWCNT. The electron diffraction patterns showed that the HNO_3-treated and nontreated MWCNTs had no significant difference either.

The MWCNT suspension, made in DMF using sonication for 1 h, was stable for 4 weeks without precipitation. A model, shown in Figure 4, suggested an interaction between the molecules of solvent DMF and the carboxylic groups attached to MWCNT surface. The interaction made the MWCNT−DMF suspension stable without any surfactant, which is usually needed for dispersing CNT. MWCNT suspension in PAN−DMF solution was ejected from a spinneret connected with a solution reservoir under a driving force of high voltage. The PAN−MWCNT composite nanofibers were formed after solvent evaporated while the jet moved from the spinneret tip to the grounded collector. The grounded moving collector, rotated at a surface speed of about 10 m/s, aligned the composite nanofibers in the nanofiber sheet, as shown in Figure 5.

3.2. Morphology of PAN−MWCNT Composite Nanofibers. SEM images (Figure 5) show that the surface morphology of the composite nanofibers is smooth at low MWCNT concentration and rougher at high concentration. That indicates that there were some MWCNTs not completely embedded into the nanofiber matrix. An AFM image (parts a and b of Figure 6) and a TEM image (Figure 6c) both confirmed that those protruded parts were the CNT segments not embedded within the nanofibers. The protruded CNT segments made the nanofiber surface rougher.

CNTs are one-dimensional nanomaterials with a nanodiameter and micron or millimeter length, which is quite a bit longer than the diameter of electrospun nanofibers. Making CNT oriented along the axes of nanofibers is a key to form CNT−polymer composite nanofibers. The electrospinning process is an effective method to produce this kind of composite nanofibers. Dror et al.[27] established a model to explain how the CNT−polymer composite nanofibers were formed by electrospinning. The MWCNT rods were randomly oriented in the electrospinning solution, but due to elongation of the fluid jet, the nanotubes were oriented along the streamlines of the electrospinning solution.

TEM is an effective tool for observation of the CNT orientation in the electrospun nanofibers since the CNT possesses a higher density compared with polymer matrix. The nanotubes containing hole structures have a darker concentric tubular structure embedded within the polymer nanofibers in the TEM image compared with the uniform matrix. Figure 7 shows a TEM image of the MWCNT embedded within the electrospun PAN−MWCNT composite nanofibers. One can clearly see the MWCNTs are well-aligned along the axis of the electrospun nanofiber by the TEM bright-field image (Figure 7b), in which CNT formed a darker image than the PAN matrix due to different densities. At higher concentration of CNT in the nanofibers,

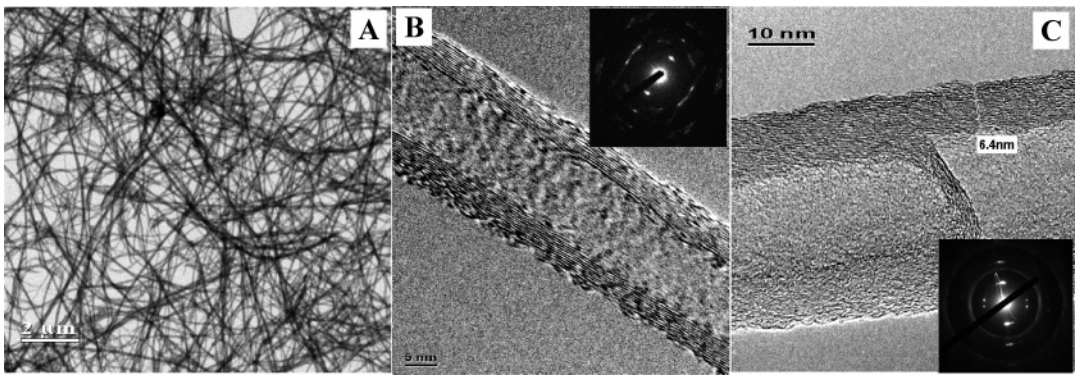

Figure 3. TEM image (A) of the MWCNT treated using 6 M HNO_3 for 12 h. (B and C) HRTEM images of the MWCNT treated and not treated using 6 M HNO_3, respectively. The inserts are the related electron diffraction patterns.

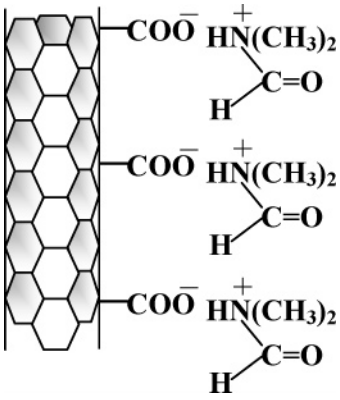

Figure 4. A diagram of the interaction model of the solvent DMF and MWCNT modified with carboxylic groups.

several CNTs were nearly parallel, loaded within a nanofiber and aligned along the axis of the nanofiber (Figure 7c).

A perfect CNT should be a straight tubular structure. However, the CNTs formed by CVD catalytic pyrolysis of hydrocarbon compound are not perfect. In most cases, the tubular structure is bent or curved to some extent, and sometimes helical since the carbon walls of the nanotubes are not completely composed of carbon hexagonal rings. Some pentagonal or heptagonal rings took the place of hexagonal rings to make the tubular structure deformed.[34] These deformed CNTs made the morphology of the electrospun CNT−polymer composite nanofibers different from that of the neat polymer electrospun nanofibers as shown in Figure 8. For a slightly curved CNT, the composite nanofiber followed the curvature of the nanotube (parts a and b of Figure 8). A highly winding or helical nanotube could not be embedded within the nanofiber by using electrospinng process (parts c and d of Figure 8). To make straight CNT−polymer composite nanofibers with smooth fiber surfaces, straight CNTs are required.

3.3. Raman Spectrum Analysis. Similar to neat MWCNTs, the MWCNTs wrapped in a PAN matrix in the composite nanofibers showed strong Raman scattering (Figure 9). The strong, sharp peak at 1577.7 cm^{-1} (G line) is assigned to the high-frequency E_{2g} first-order mode, and the strong sharp peak at 1349.9 cm^{-1} (D line) and the middle strong peak, appearing as a shoulder peak of G line, at 1612.9 cm^{-1} (D′ line) could be explained as disorder-induced features due to the finite particle size effect or lattice distortion of graphite crystals in the CNTs. The Raman scattering peak of the nitrile group (−CN) of PAN appeared at 2240 cm^{-1}. The intensity of the Raman scattering peak of nitrile group in the composite nanofibers decreased with an increase of the ratio of MWCNT in the composite nanofibers. The intensity decrease was not proportional, as shown in Figure 9.

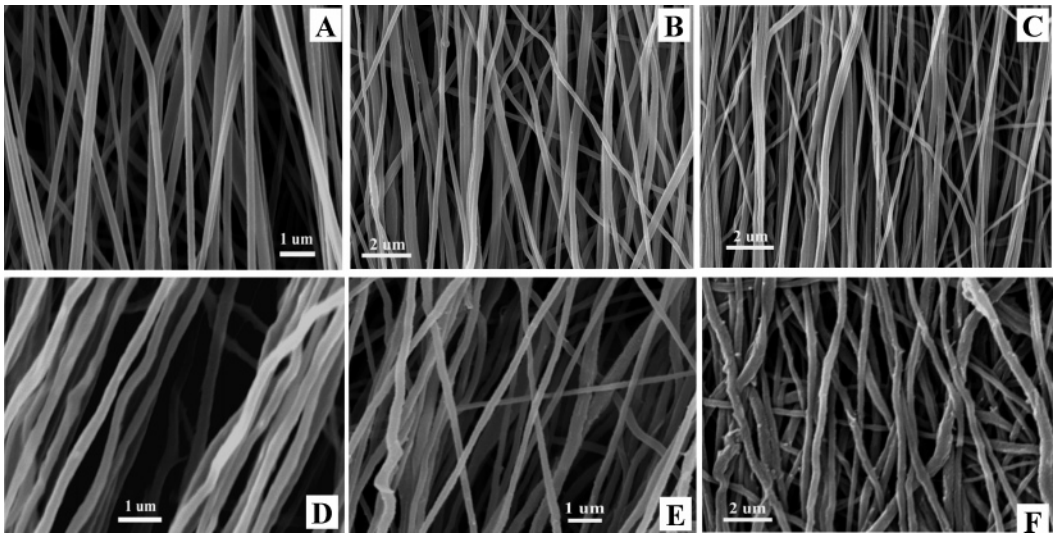

Figure 5. Scanning electron microscopic images of the aligned PAN−MWCNT composite nanofibers. (A) PAN nanofibers; (B) contains 3% MWCNT by weight; (C) 5%; (D) 10%; (E) 20%; (F) 35%.

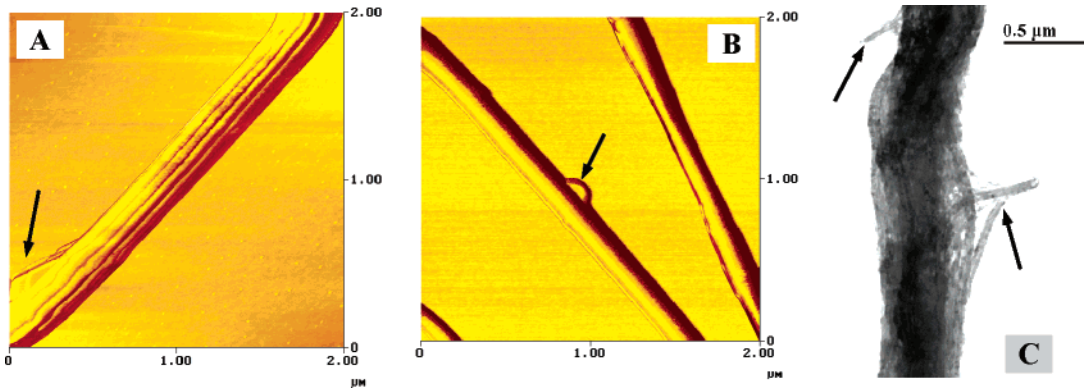

Figure 6. AFM images (A and B) made by lateral force using composite nanofiber samples containing 10 wt % MWCNT and TEM image (C) made by using the sample containing 35 wt % MWCNT. The arrows in figure point at the protruded parts of the CNT segments not embedded within the nanofibers.

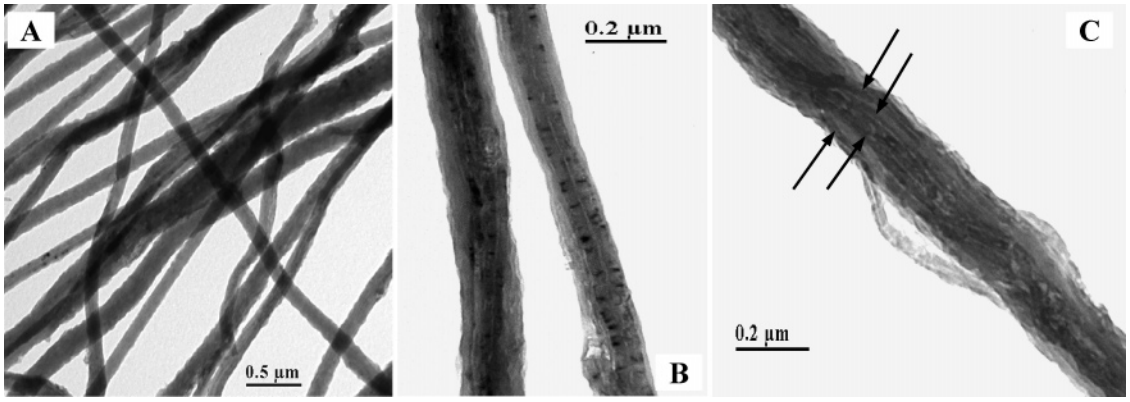

Figure 7. TEM images made using sample containing MWCNT of 10% (A and B) and 35% (C) by weight. The arrows in C point at 4 MWCNTs, respectively.

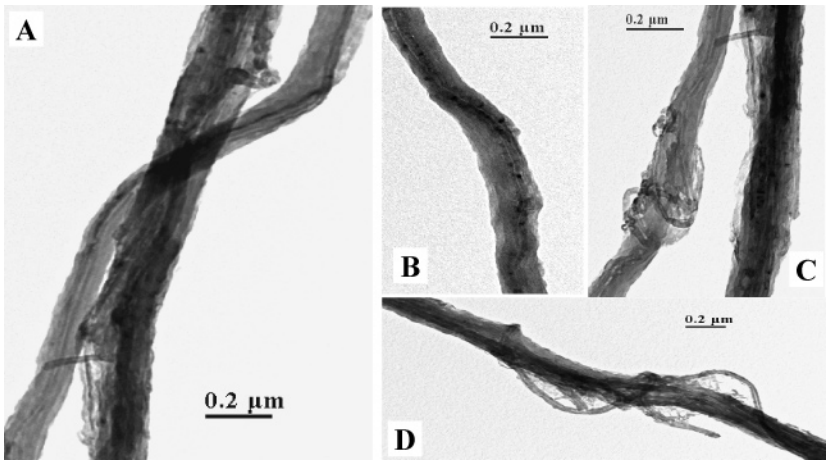

Figure 8. TEM images made using the sample containing 10 wt % (A and B) and 20 wt % (C and D) MWCNT.

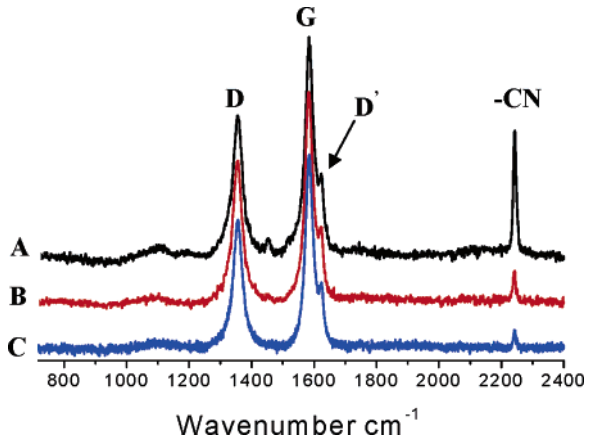

Figure 9. Raman spectra of PAN−MWCNT composite nanofiber sheets. (A), (B), and (C) contain MWCNT of 5, 10, and 20 wt %, respectively.

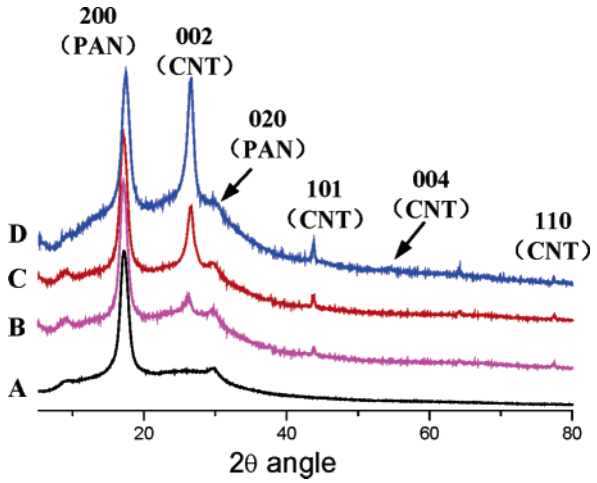

Figure 10. WAXD spectra of PAN (A) and PAN−MWCNT composite nanofiber sheets containing MWCNT of 5 (B), 10 (C), and 20% (D) by weight, respectively.

3.4. X-ray Diffraction. The WAXD spectra obtained from electrospun composite nanofiber sheets of PAN−MWCNTs are presented in Figure 10. Figure 10a is for the electrospun neat PAN nanofiber sheet. A strong peak was observed at 17.19° (2θ) and a middle strong peak at 29.95° (2θ). These two peaks of diffraction can be assigned as (200) and (020) crystal planes of PAN. Parts b−d of Figure 10 is for the electrospun composite nanofiber sheets of PAN−MWCNTs. A diffraction peak was found to become significantly stronger, compared to the diffraction peak of 200-crystal plane of PAN, as the CNT concentration increased in the composite nanofibers. The peak with significant change of intensity at 27.2° (2θ) was recognized as the diffraction of the (002) crystal planes of MWCNTs. The middle strong peak is (101) at 44.2°. The weak peaks are (004) at 54.4° and (110) at 78.6° (2θ). The result shows no significant difference from the diffraction pattern of normal MWNT.[35,36]

3.5. Mechanical Properties of Composite Nanofiber Sheets. AFM was used to evaluate the modulus of an

(34) Hou, H.; Zeng, J.; Weller, F.; Greiner, A. *Chem. Mater*. **2003**, *15*, 3170.

Table 1. Mechanical Properties of PAN−MWCNT Composite Nanofiber Sheets

no.	diameter (nm)	CNT content (%)	elongation at break (%)	tensile module (GPa)	impro. (%)	tensile strength (MPa)	impro. (%)
1	100−300	0	10.7	1.8		45.7	
2	100−300	2	9.8	2.0	11	62.9	38
3	100−300	3	8.6	2.6	44	65.7	44
4	100−300	5	2.5	3.1	72	80.0	75
5	100−300	10	1.3	3.7	106	48.6	6
6	100−300	20	0.9	4.4	144	37.1	−19

individual electrospun nanofiber segment.[28] The tensile strength and elongation at break of the nanofibers were not obtained. Stress−strain methods suitable for testing a single electrospun nanofiber were not available. The traditional stress−strain mode using stretching test could be used to evaluate the mechanical properties of the electrospun nanofiber sheet of PAN−MWCNT composite. Stretching a piece of the nanofiber sheet gives an assessment of the average mechanical properties of the composite nanofibers rather than measuring an individual segment of a composite nanofiber. Typical stress−strain curves of PAN−MWCNTs composite nanofiber sheets are presented in Figure 11. MWCNTs

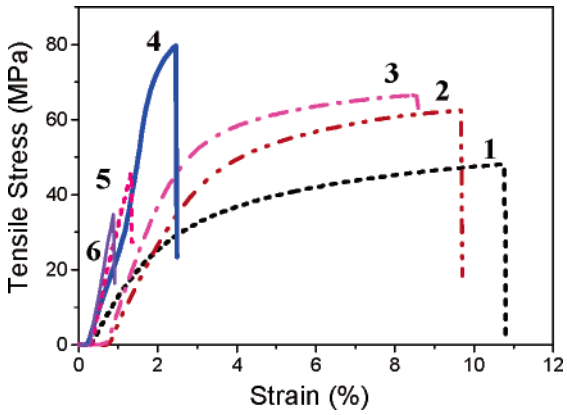

Figure 11. Typical stress−strain curves of PAN−MWCNT composite nanofiber sheets. The curves from 1 to 6 were made by using the samples containing MWCNT of 0, 2, 3, 5, 10, and 20 wt % in the composite nanofibers, respectively.

improved the modulus and tensile strength of the composite nanofiber sheet. The tensile modulus increased with increased concentration of MWCNTs in the nanofibers and reached 4.4 GPa at 20 wt % of MWCNT with a 144% improvement (see Table 1). The tensile strength showed a peak value of 80.0 MPa at about 5% MWCNT by weight with a 75% improvement. The strain to break became smaller with increase of the MWCNT concentration in the composite nanofibers.

Note that the tensile strength and E-modulus of traditional PAN (diameter more than 20 um) is normally 250−400 MPa and 3−8 GPa, respectively. The tensile strength of the PAN nanofirber sheet (Figure 11) is about 5−10 times lower than that of the traditional fiber. The small diameter of nanofiber and weak interaction between nanofibers in the nanofiber sheet may be responsible for the much lower tensile strength. Mechanically compressed (at 100 °C/3 h between two stainless steel plates) PAN nanofiber sheet exhibited a tensile strength of 265 MPa and E-modulus of 4.5 GPa[37] that matched the tensile strength and E-modulus of the traditional PAN fibers. It may be a reasonable explanation of the enhancement of the mechanical properties of the nanofiber sheet that the thermal pressure resulted in an enhancement of the interaction between nanofibers in the electrospun nanofiber sheet.

According to Ajayan's suggestion,[38] for a simple composite system without micromechanical interlocking and chemical bonding between the filler and matrix, the load transfer from a matrix to filler was realized through a weak van der Waals bonding between the filler and the matrix. For MWCNTs in PAN nanofibers, the load can be transferred from the PAN matrix to the MWCNT fillers by van der Waals bonding between the nanotubes and the matrix. The tensile strength of the composite nanofibers should increase with increased concentration of MWCNT fillers in the nanofibers. The peak value of tensile strength should not be reached at a nanotube concentration as low as 5 wt % (Table 1). Poor dispersion and poor interfacial contact of the MWCNT at higher concentration of nanotubes may be responsible for the observation that maximum tensile strength occurred at a lower concentration.

3.6. Heat Shrinkage Resistance of PAN−MWCNT Composite Nanofibers. Although the expected mechanical properties of the PAN−MWCNT composite were not obtained, a higher concentration of CNT in nanofibers did improve resistance to heat shrinkage. The heat shrinkage of the nanofiber sheet is defined as the amount that the length and width of heat-treated nanofiber sheet shrinks, expressed in terms of percentage. The heat shrinkage of PAN−MWCNT composite nanofiber sheet is presented in Figure

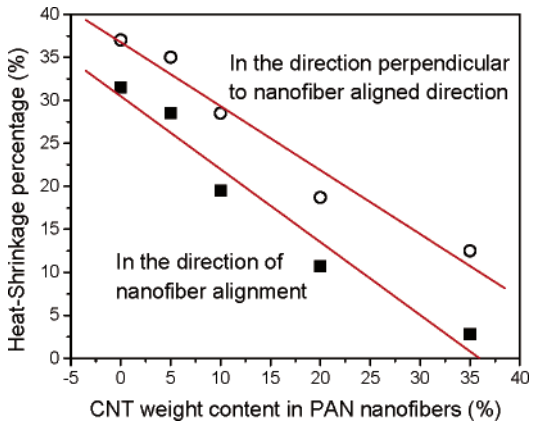

Figure 12. Diagram of heat shrinkage of composite nanofibers (the last temperature of carbonization is at 850 °C) vs CNT weight concentration in the composite nanofibers.

(35) Zhou, O.; Fleming, R. M.; Murphy, D. W.; Chen, C. H.; Haddon, R. C.; Ramirez, A. P.; Glarum, S. H. *Science* **1994**, *263*, 1744.
(36) Cao, A.; Xu, C.; Liang, J.; Wu, D.; Wei, B. *Chem. Phys. Lett.* **2001**, *344*, 13.

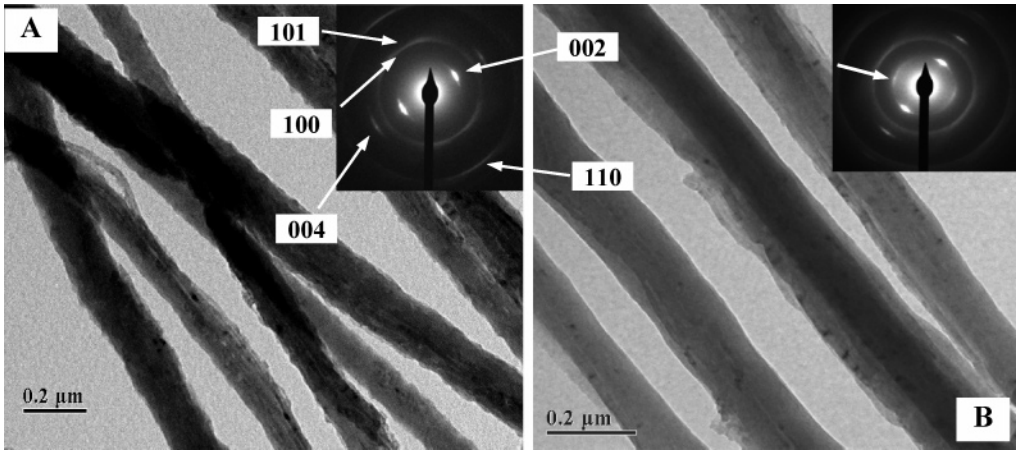

Figure 13. TEM images of as-formed (A) and carbonized (B) PAN−MWCNT composite nanofibers. The inserts are the related electron diffraction patterns

12. The composite nanofibers containing 35 wt % MWCNTs showed a much smaller heat shrinkage in the direction of nanofiber alignment from room temperature to 850 °C due to the fact that carbon nanotubes do not shrink. During the course of heating from room temperature to 850 °C in an inert atmosphere, the PAN matrix was carbonized to turbostratic graphite packed around the carbon nanotubes. The morphology and shape of the composite nanofibers were maintained after the carbonization process (Figure 13). The inserted electron diffraction pattern of Figure 13b showed that the newly formed carbon material was disordered graphite. The arrowed pattern of the insert of Figure 13b should be attributed to the diffraction pattern contributed by 002 crystal planes of the newly formed carbon structure. The packing density of the carbonized matrix molecules around the MWCNT seemed to become almost the same density of the CNT filler by comparing the TEM images of a carbonized composite nanofiber and a non-carbonized composite nanofiber (parts a and b of Figure 14).

4. Conclusion

In summary, PAN−MWCNT composite sheets of aligned nanofibers containing different concentrations of MWCNTs were made in large amounts by electrospinning. MWCNTs were oriented along the axes of the nanofibers and were nearly parallel in each electrospun nanofiber. Raman spectrum analysis showed that the MWCNTs embedded in a PAN matrix showed a strong Raman scattering with less dependence on MWCNT concentration in the composite nanofibers. X-ray diffraction depends on MWCNT concentration. MWCNTs reinforced the PAN nanofibers and improved the tensile modulus by 144% at 20% MWCNTs by weight, and the tensile strength by 75% at 5% MWCNTs. The morphology and shape of the PAN−MWCNT composite nanofiber were maintained after carbonization process. The heat shrinkage of the composite nanofiber sheet was effectively reduced during the course of carbonization. For a CNT concentration of 35%, the sample shrank only 3% in the direction of nanofiber alignment and only 11% in the direction perpendicular to nanofiber alignment.

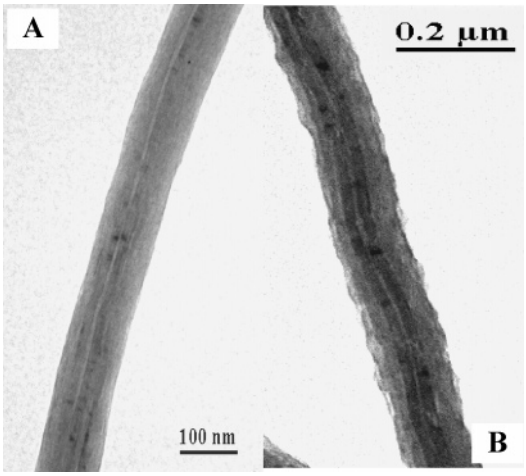

Figure 14. TEM images of carbonized PAN−MWCNT composite nanofibers (A) and as-formed PAN-MWCNT composite nanofibers (B).

Acknowledgment. The authors are indebted to Dr. Frank Weller (Chemistry Department of Philipps−University Marburg) for Raman spectrum measurements of the samples and to NSFC and to the Chinese Ministry of Science and Technology for financial supports (NSFC Grant 20464001 and "973" Great Fundamental Research Grant 2004CCA04700).

CM0484955

(37) Ge, J. J.; Hou, H.; Li, Q.; Graham, M.; Greiner, A.; Reneker, D. H.; Harris, F. W.; Cheng, S. Z. D. *J. Am. Chem. Soc.* **2004**, *126*, 15754.
(38) Schadler, L. S.; Giannaris, S. C.; Ajayan, P. M. *Applied Physics Lett.* **1998**, *73* (26), 3842.